Eur. Phys. J. D **7**, 399–412 (1999)

THE EUROPEAN PHYSICAL JOURNAL D

EDP Sciences
© Società Italiana di Fisica
Springer-Verlag 1999

Bose-Einstein condensates with vortices in rotating traps

Y. Castin[1,a] and R. Dum[1,2]

[1] Laboratoire Kastler Brossel[b], École Normale Supérieure, 24 rue Lhomond, 75231 Paris Cedex 05, France
[2] Institut d'Optique, Université Paris-Sud, bâtiment 503, B.P. 147, 91403 Orsay Cedex, France

Received 16 December 1998 and Received in final form 18 March 1999

Abstract. We investigate minimal energy solutions with vortices for an interacting Bose-Einstein condensate in a rotating trap. The atoms are strongly confined along the axis of rotation z, leading to an effective 2D situation in the $x-y$ plane. We first use a simple numerical algorithm converging to local minima of energy. Inspired by the numerical results we present a variational ansatz in the regime where the interaction energy per particle is stronger than the quantum of vibration in the harmonic trap in the $x-y$ plane, the so-called Thomas-Fermi regime. This ansatz allows an easy calculation of the energy of the vortices as function of the rotation frequency of the trap; it gives a physical understanding of the stabilisation of vortices by rotation of the trap and of the spatial arrangement of vortex cores. We also present analytical results concerning the possibility of detecting vortices by a time-of-flight measurement or by interference effects. In the final section we give numerical results for a 3D configuration.

PACS. 03.75.Fi Phase coherent atomic ensembles; quantum condensation phenomena – 67.40.Vs Vortices and turbulence – 32.80.Pj Optical cooling of atoms; trapping

1 Introduction

After the achievement of Bose-Einstein condensates in trapped atomic gases [1] many properties of these systems have been studied experimentally and theoretically [2]. However a striking feature of superfluid helium, quantized vortices [3,4], has not yet been observed in trapped atomic gases. There is an abundant literature on vortices in helium II, an overview is given in [4].

The atomic gases have interesting properties which justify efforts to generate vortices in these systems: the core size of the vortices is adjustable, as in contrast to helium the strength of the interaction can be adjusted through the density; the number of vortices in atomic gases can be in principle well-controlled; for a small number of particles in the gas metastability of the vortices can be studied, that is one can watch spontaneous transitions between configurations with different number of vortices.

Several ways to create vortices in atomic gases have been suggested. A method inspired from liquid helium consists in rotating the trap confining the atoms [5]; at a large enough rotation frequency it becomes energetically favorable at low temperatures to produce vortices; two different paths could be in principle followed: (1) producing first a condensate then rotating the trap, or (2) cooling the gas directly in a rotating trap. It has been recently proposed in [6] to use quantum topological effects to obtain a vortex. Other methods that do not rely on thermal equilibrium have been suggested [7,8].

Here we study theoretically the minimal energy configurations of vortices in a rotating trap [9]. The model is defined in Section 2; in Sections 3 to 6 we assume a strong confinement of the atoms along the rotation axis z so that we face an effective 2D problem in the transverse plane $x-y$. We present numerical results for solutions with vortices that are local minima of the Gross-Pitaevskii energy functional (Sect. 3). These solutions contain only vortices with a charge ± 1, the vortices with a charge larger than or equal to 2 are thermodynamically unstable (Sect. 4). We discuss possibilities to get experimental evidence of vortices in atomic gases in Section 5. Finally, we concentrate on the regime where the interaction energy is much larger than the trap frequencies $\omega_{x,y}$, the so-called Thomas-Fermi limit [2]. This is complementary to the work of [10]. We obtain in this "strong interacting" regime analytical predictions based on a variational ansatz that reproduce satisfactorily the numerical results (Sect. 6). In Section 7 we present results for vortices in 3D, that is in a trap with a weak confinement along the rotation axis.

2 Model considered in this paper

The atoms are trapped in a potential rotating at angular velocity Ω. In the laboratory frame the Hamiltonian of the gas is therefore time dependent. To eliminate

[a] e-mail: castin@physique.ens.fr
[b] Unité de recherche de l'École Normale Supérieure et de l'Université Pierre et Marie Curie, associée au CNRS.

this time dependence we introduce a rotating frame at the angular velocity Ω so that the trapping potential becomes time independent; this change of frame is achieved by the single-atom unitary transform:

$$\mathcal{U}(t) = \mathrm{e}^{\mathrm{i}\boldsymbol{\Omega}\cdot\mathbf{L}t/\hbar} \tag{1}$$

where $\mathbf{L}$ is the angular momentum operator of a single atom. As the unitary transform is time dependent the Hamiltonian in the rotating frame contains an extra inertial term, given for each atom by

$$\mathrm{i}\hbar\mathcal{U}^\dagger(t)\frac{\mathrm{d}}{\mathrm{d}t}\mathcal{U}(t) = -\boldsymbol{\Omega}\cdot\mathbf{L}. \tag{2}$$

The atoms are interacting via the effective low energy potential commonly considered in the literature, $V(\mathbf{r}_1-\mathbf{r}_2) = g_{3\mathrm{D}}\delta(\mathbf{r}_1-\mathbf{r}_2)$, where the coupling constant is related to the s-wave scattering length a (taken here to be positive) and to the atomic mass m by $g_{3\mathrm{D}} = 4\pi\hbar^2 a/m$. In this paper we consider the case of a dilute gas (with a density much smaller than a^{-3}) at zero temperature. We can then assume that the N particles of the gas are condensed in the same state ϕ. The wavefunction $\phi(\mathbf{r})$ is time independent as we are in the rotating frame and minimizes the energy per particle in the condensate, given by the Ginzburg-Landau energy functional:

$$E[\phi,\phi^*] = \int \mathrm{d}^3\mathbf{r}\ \frac{\phi^*(\mathbf{r})\,[\mathcal{H}_0 - \boldsymbol{\Omega}\cdot\mathbf{L}]\,\phi(\mathbf{r})}{\langle\phi|\phi\rangle} + \frac{1}{2}\frac{Ng_{3\mathrm{D}}|\phi|^4}{\langle\phi|\phi\rangle^2}\,. \tag{3}$$

In this energy functional $\mathcal{H}_0$ contains the kinetic energy and the trapping potential energy of the particles:

$$\mathcal{H}_0 = -\frac{\hbar^2}{2m}\Delta + U(\mathbf{r}, t=0). \tag{4}$$

The energy functional includes also the inertial term $-\boldsymbol{\Omega}\cdot\mathbf{L}$ and a term proportional to $|\phi|^4$ describing the interaction energy between the particles in the mean field approximation.

As done in the present experiments with atomic gases we take the case of a harmonic trap, with eigenfrequencies ω_α:

$$U(\mathbf{r}, t=0) = \sum_{\alpha=x,y,z}\frac{1}{2}m\omega_\alpha^2 r_\alpha^2. \tag{5}$$

Furthermore in all but in Section 7 we will assume that the trapping potential is much stronger along the z axis than along the x, y axis, with an oscillation frequency much larger than the typical interaction energy $Ng_{3\mathrm{D}}|\phi|^2$ per particle. This situation, although not realized experimentally yet, is not out of reach, in particular when one uses optical traps rather than magnetic traps [11]. In this strong confining regime the motion of the particles along z is frozen in the ground state of the strong harmonic potential:

$$\phi(x,y,z) \simeq \psi(x,y)\left(\frac{m\omega_z}{\pi\hbar}\right)^{1/4}\mathrm{e}^{-m\omega_z z^2/2\hbar} \tag{6}$$

and only the dependence of the wavefunction ψ in the $x-y$ plane remains to be determined. Inserting equation (6) in the energy functional equation (3) we get the corresponding energy functional for ψ to be minimized, dropping the constant term $(1/2)\hbar\omega_z$:

$$E[\psi,\psi^*] = \int \mathrm{d}^2\mathbf{r}\ \frac{\psi^*(\mathbf{r})\,[\mathcal{H}_\perp - \Omega L_z]\,\psi(\mathbf{r})}{\langle\psi|\psi\rangle} + \frac{1}{2}\frac{Ng|\psi|^4}{\langle\psi|\psi\rangle^2}\,. \tag{7}$$

This 2D energy functional gives the energy per particle in the condensate measured from the zero-point energy along z. The 2D Hamiltonian is

$$\mathcal{H}_\perp = -\frac{\hbar^2}{2m}\Delta_{x,y} + \frac{1}{2}\sum_{\alpha=x,y} m\omega_\alpha^2 r_\alpha^2. \tag{8}$$

The trap is now rotated around the z axis at the angular velocity Ω. The interaction term $|\psi|^4$ involves an effective 2D coupling constant between the atoms [12]

$$g = g_{3\mathrm{D}}\left(\frac{m\omega_z}{2\pi\hbar}\right)^{1/2}. \tag{9}$$

Most of the results of the paper are dealing with the 2D energy functional; a numerical result for a local minimum of the full 3D energy functional will be given in the Section 7. We concentrate on the so-called Thomas-Fermi regime, where the interaction energy per particle is much larger than $\hbar\omega_{x,y}$. The opposite regime has already been studied in [10].

3 Local minima of energy with vortices

In this section we briefly discuss the general problem of minimizing energy functionals of the type equation (7). We present the numerical algorithm that we have used and we give numerical results for the 2D problem.

3.1 A numerical algorithm to find local minima

The algorithm in our numerical calculations is commonly used in the literature to minimize energy functionals $E[\psi,\psi^*]$ of the form equation (7). The intuitive idea is to start from a random ψ and move it opposite to the local gradient of $E[\psi,\psi^*]$ that is along the local downhill slope of the energy. Numerically this is implemented by an evolution of ψ parametrized by a fictitious time τ:

$$-\frac{\mathrm{d}}{\mathrm{d}\tau}\psi = \frac{\delta E}{\delta\psi^*}[\psi,\psi^*]. \tag{10}$$

Assuming a ψ normalized to unity we get the following equation of motion for ψ:

$$-\frac{\mathrm{d}}{\mathrm{d}\tau}\psi = [\mathcal{H}_\perp - \Omega L_z + Ng|\psi|^2 - \mu(\tau)]\psi \tag{11}$$

that is a non-linear Schrödinger equation in complex time $t = -\mathrm{i}\tau$. The quantity μ appearing in this equation can

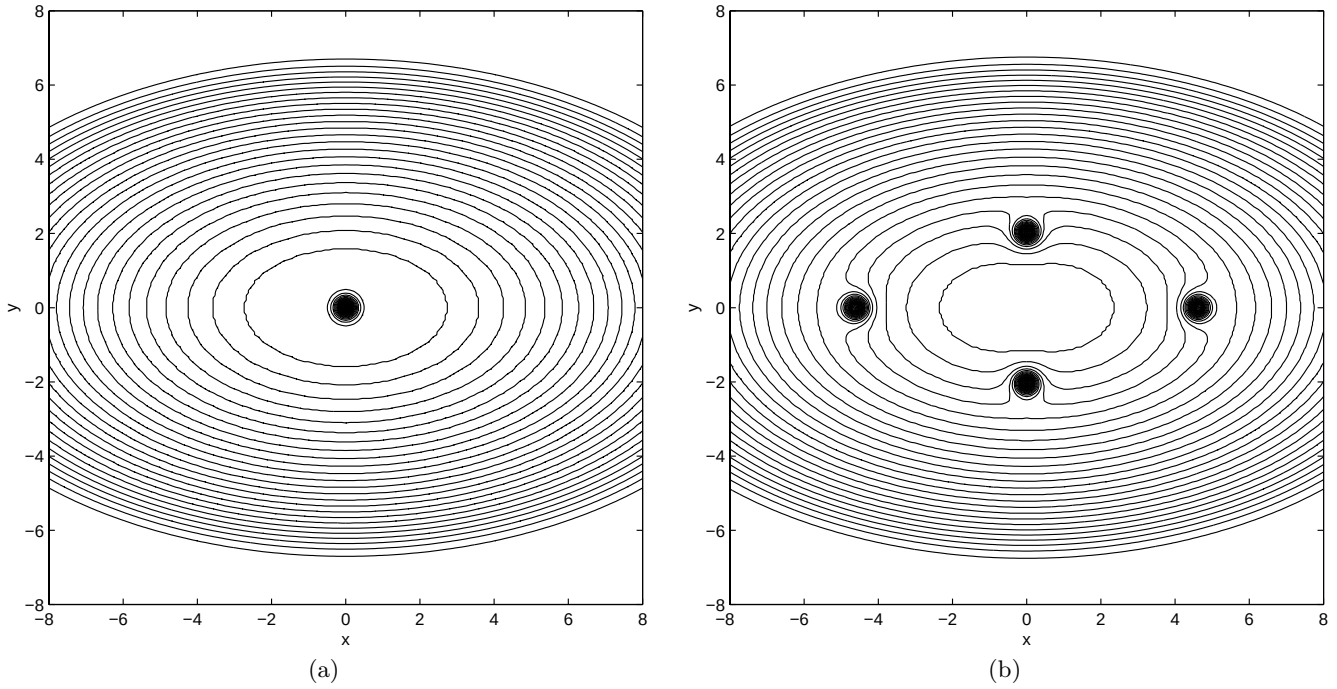

Fig. 1. Isocontours of the density $|\psi|^2$ for a 1-vortex (a) and a 4-vortex (b) configuration obtained numerically in a non-axisymmetric trap ($\epsilon = 0.3$) with a rotation frequency $\Omega = 0.2\omega$, and $\mu \simeq 40\hbar\omega$ (see text for the definition of ϵ, ω); the unit of length for x and y is $(\hbar/m\omega)^{1/2}$.

be expressed explicitly in terms of a functional of ψ, ψ^*; it ensures that the norm of ψ does not evolve with τ.

This equation is, for $\Omega = 0$, standardly solved by a splitting technique, propagating during the time step $\mathrm{d}\tau$ first with potential energy in position space (where it is diagonal) then with kinetic energy in momentum space (where the Laplacian is diagonal). One goes back and forth between position and momentum space with Fast Fourier Transforms along x and y. In our case $\Omega \neq 0$ and the Hamiltonian contains $L_z = xp_y - yp_x$; we have therefore complemented the splitting scheme by (1) a propagation during $\mathrm{d}\tau$ due to $-\hbar\Omega x p_y$ in position space along x and momentum space along p_y, and (2) a similar procedure for the $\hbar\Omega y p_x$ propagation, that is in momentum space along x and position space along y.

One can check that the mean energy of ψ is a decreasing function of τ:

$$\frac{\mathrm{d}}{\mathrm{d}\tau} E[\psi, \psi^*] = -2 \int \mathrm{d}^2\mathbf{r} \left| \frac{\delta E}{\delta \psi^*} \right|^2 \leq 0. \qquad (12)$$

In the case we consider E remains always positive: the scattering length and therefore g are positive so that the interaction term is positive, and $|\Omega|$ is smaller than the trap frequencies $\omega_{x,y}$ so that the centrifugal potential $-m\Omega^2 r^2/2$ cannot exceed the trapping potential. Therefore E has to converge to a finite value for $\tau \to \infty$. Asymptotically $\mathrm{d}E/\mathrm{d}\tau = 0$ and ψ satisfies $\delta E/\delta\psi^*[\psi, \psi^*] = 0$, so that we recover for $\tau = \infty$ the time independent Gross-Pitaevskii equation:

$$\mu\psi = \mathcal{H}_\perp \psi + Ng|\psi|^2\psi - \Omega L_z \psi \qquad (13)$$

where $\mu = \mu(\tau = \infty)$ is now the chemical potential of the gas [2].

As we have started from a random wavefunction ψ, without assuming any symmetry properties of ψ, we expect the trajectory $\psi(\tau)$ to converge as $\tau \to \infty$ to a local minimum of the energy functional. We have checked this assumption by adding a small random wavefunction to ψ and resuming the evolution in τ; ψ was relaxing to its initial value. Mathematically the steady state solutions for the τ evolution that we find are stable, which is equivalent to saying that they are local minima of the energy. Note that not all solutions of the Gross-Pitaevskii equation share this property: the Gross-Pitaevskii equation expresses only the fact that the energy functional is stationary in ψ, which is the case *e.g.* at saddle points of the energy functional (an example is a vortex with a charge $|q| > 1$, see Sect. 4).

3.2 Numerical results in 2D

Applying the algorithm detailed in the previous section we present results on local minima of the energy functional equation (7) for asymmetric and symmetric traps in the $x-y$ plane. We characterize the non-axisymmetry of the trap by ϵ such that

$$\omega_x = \omega/(1+\epsilon) \qquad (14)$$

$$\omega_y = \omega(1+\epsilon). \qquad (15)$$

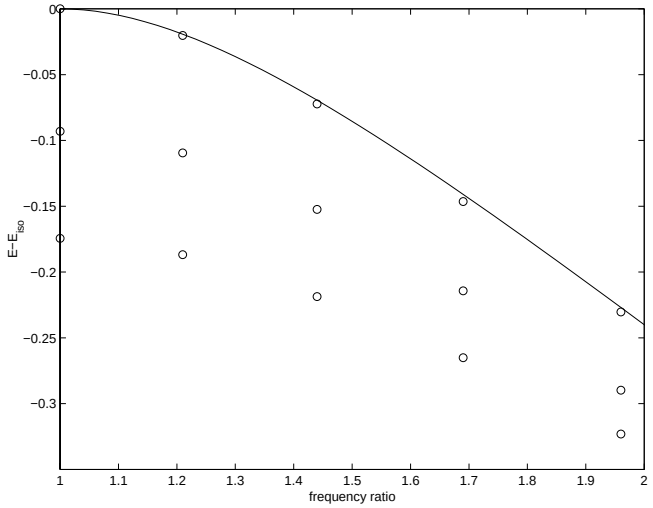

Fig. 2. Numerical results for the energy of 0-vortex, 1-vortex and 4-vortex configurations (from top to bottom), as function of the frequency ratio ω_x/ω_y, for a fixed product of the frequencies $\omega^2 = \omega_x\omega_y$. The rotation frequency of the trap is $\Omega = 0.2\omega$ and the energies are measured in units of $\hbar\omega$ from the 0-vortex energy $E_{\rm iso}$ in the axi-symmetric trap; the chemical potential is $\mu \simeq 40\hbar\omega$. The circles correspond to numerical results; the solid line is an analytical prediction for the 0-vortex case as obtained in Section 6.2.

In Figure 1 we show different local minima configurations obtained for $\epsilon = 0.3$ and a rotation frequency $\Omega = 0.2\omega$; each configuration has been obtained for different random initial ψ's. The holes observed in the spatial density correspond to the vortex cores. We have always found that the phase of ψ changes by 2π around a vortex core; we have not found vortices with a charge $\pm q$, where the integer q is strictly larger than one; this fact will be explained in the next section. Furthermore the sense of circulation is the same for all vortices.

To quantify the effect of the non-axisymmetry of the trap we have plotted in Figure 2 the dependence of energy of different vortex configurations on ω_x/ω_y for a fixed ω; we measure the energies from $E_{\rm iso}$, the energy of the zero-vortex solution in the axisymmetric case $\epsilon = 0$. The zero-vortex solution exhibits a significant variation of energy with ϵ; for a non-zero ϵ the wavefunction ψ develops a phase proportional to Ω for weak Ω's, which accounts for the energy change as explained in Section 6.2. The solutions with vortices experience quasi the same energy shift as function of ϵ. As only the energy difference between the various local minima matters we will from now on only consider the axisymmetric case $\epsilon = 0$ to identify the solution with the absolute minimal energy.

Note that the solutions ψ with several vortices obtained in the limiting case $\epsilon = 0$ are not eigenvectors of L_z; this reflects a general property of non-linear equations such as the Gross-Pitaevskii equations to have *symmetry broken solutions*; it is explained in [10] how to reconcile this symmetry breaking with the fact that eigenvectors of the full N-atom Hamiltonian are of well-defined angular momentum.

4 Stability properties of vortices

In this section we recall that a (normalized) wavefunction ψ such that $E[\psi, \psi^*]$ has a local minimum in ψ, describes a condensate having all the desired properties of stability, that is dynamical and thermodynamical stability. We then show that a vortex centered at $\mathbf{r} = \mathbf{0}$ with an angular momentum strictly larger than $\hbar$ is not a local minimum of energy and is therefore thermodynamically unstable.

4.1 Stability properties of local minima

Let us express the fact that ψ corresponds to a local minimum of the energy. A first condition is that the energy functional is stationary for ψ, that is ψ solves the Gross-Pitaevskii equation equation (13). To get the second condition, we consider a small variation of ψ,

$$\psi \to \psi + \delta\psi \tag{16}$$

preserving the normalization of the condensate wavefunction to unity:

$$||\psi + \delta\psi||^2 - ||\psi||^2 = 0 = \langle\psi|\delta\psi\rangle + \langle\delta\psi|\psi\rangle + \langle\delta\psi|\delta\psi\rangle. \tag{17}$$

We expand the energy functional $E[\psi, \psi^*]$ in powers of $\delta\psi$, neglecting terms of order $\delta\psi^3$ or higher. Using equations (17, 13) we find that terms linear in $\delta\psi$ vanish so that

$$\delta E = \frac{1}{2}(\langle\delta\psi|, \langle\delta\psi^*|)\mathcal{L}_{\rm c}\begin{pmatrix}|\delta\psi\rangle\\ |\delta\psi^*\rangle\end{pmatrix} + o(\delta\psi^2). \tag{18}$$

We have introduced the operator

$$\mathcal{L}_{\rm c} = \begin{pmatrix}\mathcal{H}_{\rm GP} + Ng|\psi|^2 & Ng\psi^2\\ Ng\psi^{*^2} & \mathcal{H}^*_{\rm GP} + Ng|\psi|^2\end{pmatrix} \tag{19}$$

and the Gross-Pitaevskii Hamiltonian

$$\mathcal{H}_{\rm GP} = \mathcal{H}_\perp + Ng|\psi|^2 - \Omega L_z - \mu. \tag{20}$$

The fact that E has a local minimum in ψ imposes that the Hermitian operator $\mathcal{L}_{\rm c}$ be positive. In general $\mathcal{L}_{\rm c}$ will be strictly positive apart from the zero energy mode $({\rm i}\psi, -{\rm i}\psi^*)$ corresponding to an inessential change of the global phase of ψ. We now show that the positivity of $\mathcal{L}_{\rm c}$ implies the stability of the solution ψ.

4.1.1 Dynamical stability

Consider first the problem of so-called "dynamical stability": to be a physically acceptable condensate wavefunction, ψ has to be a stable solution of the time dependent Gross-Pitaevskii equation

$${\rm i}\hbar\partial_t\psi = \mathcal{H}_{\rm GP}\psi \tag{21}$$

otherwise any small perturbation of ψ, *e.g.* the effect of quantum fluctuations or experimental noise, may lead to an evolution of ψ far from its initial value. To determine the evolution of a small deviation $\delta\psi$ as in equation (16) we linearize equation (21):

$$\mathrm{i}\hbar\partial_t \begin{pmatrix} |\delta\psi\rangle \\ |\delta\psi^*\rangle \end{pmatrix} = \mathcal{L} \begin{pmatrix} |\delta\psi\rangle \\ |\delta\psi^*\rangle \end{pmatrix} \tag{22}$$

where the operator $\mathcal{L}$ is related to $\mathcal{L}_{\rm c}$ by

$$\mathcal{L}_{\rm c} = \begin{pmatrix} 1 & 0 \\ 0 & -1 \end{pmatrix} \mathcal{L}. \tag{23}$$

As ψ is time independent, so is $\mathcal{L}$ and dynamical stability is equivalent to the requirement that the eigenvalues of $\mathcal{L}$ have all a negative or vanishing imaginary part. As we now show the positivity of $\mathcal{L}_{\rm c}$ leads to a purely real spectrum for $\mathcal{L}$. Consider an eigenvector (u, v) of $\mathcal{L}$ with the eigenvalue ε. Contracting equation (23) between the ket $(|u\rangle, |v\rangle)$ and the bra $(\langle u|, \langle v|)$ we get

$$\varepsilon\left[\langle u|u\rangle - \langle v|v\rangle\right] = (\langle u|, \langle v|)\mathcal{L}_{\rm c} \begin{pmatrix} |u\rangle \\ |v\rangle \end{pmatrix}. \tag{24}$$

Note that the matrix element of $\mathcal{L}_{\rm c}$ is real positive as $\mathcal{L}_{\rm c}$ is a positive hermitian operator. We now face two possible cases for the real quantity $\langle u|u\rangle - \langle v|v\rangle$:

- $\langle u|u\rangle - \langle v|v\rangle = 0$. In this case $\mathcal{L}_{\rm c}$ has a vanishing expectation value in $(|u\rangle, |v\rangle)$; as $\mathcal{L}_{\rm c}$ is positive $(|u\rangle, |v\rangle)$ has to be an eigenvector of $\mathcal{L}_{\rm c}$ with the eigenvalue zero; from equation (23) and the fact that $\begin{pmatrix} 1 & 0 \\ 0 & -1 \end{pmatrix}$ is invertible we find that $(|u\rangle, |v\rangle)$ is also an eigenvalue of $\mathcal{L}$ with the eigenvalue 0, so that $\varepsilon = 0$ is a real number;
- $\langle u|u\rangle - \langle v|v\rangle > 0$: we get ε as the ratio of two real numbers, so that ε is real.

4.1.2 Thermodynamical stability

A second criterion of stability is the so-called "thermodynamical" stability. For zero temperature, this condition can be formulated in the Bogoliubov approach [2], where the particles out of the condensate, which always exist because of the interactions, are described by a set of uncoupled harmonic oscillators with frequencies $\varepsilon\mathrm{sign}\left[\langle u|u\rangle - \langle v|v\rangle\right]/\hbar$, where (u, v) is an eigenvector of $\mathcal{L}$ with the eigenvalue ε. In order for a thermal equilibrium to exist for these oscillators, their frequencies should be strictly positive, which is the case here in virtue of equation (24) [13]. If a mode with a negative frequency were present thermalization by collisions would transfer particles from the condensate ψ to this mode, leading to a possible evolution of the system far from the initial state ψ [14].

What happens for solutions ψ of the Gross-Pitaevskii equations that are not local minima of energy? The operator $\mathcal{L}_{\rm c}$ has at least an eigenvector with a strictly negative eigenvalue. In this case one cannot have thermodynamical stability, that is one cannot have $\varepsilon\left[\langle u|u\rangle - \langle v|v\rangle\right] > 0$ for all modes [13]. From the non-positivity of $\mathcal{L}_{\rm c}$ one cannot however distinguish between a simple thermodynamically instability or a more dramatic dynamical instability.

4.2 Why not a vortex of angular momentum larger than $\hbar$?

For simplicity we consider only a single vortex in the center of an axi-symmetric trap. We show that vortices with a change of phase of $2q\pi$ are not local minima of energy, that is are (at least thermodynamically) unstable. We have found numerically a solution of the Gross-Pitaevskii equation equation (13) by an evolution in complex time, starting from a wavefunction ψ with an angular momentum $q\hbar$ along z, as already done in [15]; our solution of the Gross-Pitaevskii equation with imposed symmetry is a local minimum of energy in the subspace of functions with angular momentum $q\hbar$ along z, but not necessarily a local minimum in the whole functional space, as we will see for $|q| > 1$. In the Thomas-Fermi regime $\mu \gg \hbar\omega$ we find that the solutions can be well-reproduced by a variational ansatz of the form

$$\psi(x, y) = \mathrm{e}^{\mathrm{i}q\theta}\left[\tanh\kappa_q r\right]^{|q|}\left(\frac{\tilde{\mu} - m\omega^2 r^2/2}{Ng}\right)^{1/2} \tag{25}$$

where θ is the polar angle in the $x-y$ plane and where $\tilde{\mu}$, the chemical potential in the lab frame

$$\tilde{\mu} = \mu + q\hbar\Omega \tag{26}$$

does not depend on Ω. In this ansatz the vortex core is accounted for by $\tanh^{|q|}$, a function that vanishes as $r^{|q|}$ in zero as it should, and the condensate density outside the core coincides with the Thomas-Fermi approximation commonly used for the zero-vortex solution [2]. We calculate the mean energy equation (7) of the variational ansatz and we minimize it with respect to the variational parameter κ_q; we get

$$\kappa_q = \left[\frac{\tilde{\mu}m}{\hbar^2}\right]^{1/2} c_q \tag{27}$$

where

$$c_q^2 = \frac{2}{q^2}\int_0^{+\infty} \mathrm{d}u\; u\left(\tanh^{2|q|}(u) - 1\right)^2 \tag{28}$$

is a number ($c_1 = 0.7687, c_2 = 0.5349, \ldots$).

In order for the vortex of charge q to be a local minimum of energy, the operator $\mathcal{L}_{\rm c}$ of equation (19) has to be positive. This implies that the operator on the first line, first column of $\mathcal{L}_{\rm c}$, the so-called Hartree-Fock Hamiltonian, be positive:

$$\mathcal{H}_{\rm HF} = \mathcal{H}_\perp + 2Ng|\psi|^2 - \tilde{\mu} + q\hbar\Omega - \Omega L_z \geq 0. \tag{29}$$

To show that this is not the case it is sufficient to find a wavefunction $f(x,y)$ leading to a negative expectation value for $\mathcal{H}_{\rm HF}$. As the potential appearing in $\mathcal{H}_{\rm HF}$ has a dip at $r=0$ we have taken f of a form localized around $r=0$:

$$f(x,y)=\frac{1}{\cosh\left[\gamma\left(\frac{\tilde{\mu}m}{\hbar^2}\right)^{1/2}r\right]} \tag{30}$$

where γ is adjusted to minimize the expectation value. For *e.g.* $q=2$ we take $\gamma=1$ leading to

$$\frac{\langle f|H_{\rm HF}|f\rangle}{\langle f|f\rangle}\simeq -0.407\tilde{\mu}+2\hbar\Omega. \tag{31}$$

As $\Omega<\omega\ll\mu$ this quantity is negative. A similar conclusion is obtained for $q>2$.

We have also performed a numerical experiment, evolving ψ in complex time starting from equation (25); we find that the vortex $q=2$ splits in two vortices $q=+1$ symmetrically dispatched [14]. A numerical diagonalization of $\mathcal{L}$ shows that the vortex $q=2$ is alternatively dynamically and thermodynamically unstable when one increases $\tilde{\mu}/\hbar\omega$ [16].

5 How to detect the presence of vortices?

Several signatures of the presence of vortices have been proposed in the literature. A first possibility is a measurement of the excitation spectrum as studied in [17]. Another idea is to measure the second order correlation function of the atomic field [18].

A third signature of the presence of vortices is also the holes in the density due to the vortex cores. As the size of the vortex core in the Thomas-Fermi regime is too small to be observed *in situ* by optical imaging techniques, we suggest to switch off the trapping potential and let the cloud expand; as we now check the size of the cloud and the size of the vortex cores are magnified by the same factor in the expansion, so that the cores become observable.

To study the expansion of the gas when the trap in the $x-y$ plane is switched off, the confinement along z being kept constant, one has to solve a 2D time dependent Gross-Pitaevskii equation. In this section the trap is axi-symmetry with a time dependent frequency $\omega(t)$. We consider the evolution in the laboratory frame, as the detection is performed in this frame:

$$\mathrm{i}\hbar\partial_t\psi_{\rm lab}=\left[-\frac{\hbar^2}{2m}\Delta+\frac{1}{2}m\omega^2(t)r^2+Ng|\psi_{\rm lab}|^2\right]\psi_{\rm lab}. \tag{32}$$

As shown in [19,20] the effect of the time dependence of $\omega(t)$ can be absorbed by a scaling and gauge transform of the wavefunction:

$$\psi_{\rm lab}(\mathbf{r},t)=\frac{1}{\lambda(t)}\mathrm{e}^{\mathrm{i}mr^2\dot{\lambda}/2\hbar\lambda}\tilde{\psi}(\mathbf{r}/\lambda(t),t) \tag{33}$$

where $\omega(0)$ is the oscillation frequency before opening the trap; the scaling parameter solves:

$$\ddot{\lambda}=\frac{\omega^2(0)}{\lambda^3}-\omega^2(t)\lambda \tag{34}$$

with initial conditions $\lambda(0)=1,\dot{\lambda}(0)=0$; if the trap in the $x-y$ plane is abruptly switched off at $t=0^+$ the scaling parameter is given by

$$\lambda(t)=\sqrt{1+\omega^2(0)t^2}. \tag{35}$$

Introducing the renormalized time τ given by

$$\frac{\mathrm{d}t}{\lambda^2(t)}=\mathrm{d}\tau \tag{36}$$

we find that $\tilde{\psi}$ solves the same equation as $\psi_{\rm lab}$ with a *constant* trap frequency equal to $\omega(0)$:

$$\mathrm{i}\hbar\partial_\tau\tilde{\psi}=\left[-\frac{\hbar^2}{2m}\Delta+\frac{1}{2}m\omega^2(0)r^2+Ng|\tilde{\psi}|^2\right]\tilde{\psi}. \tag{37}$$

As $\psi_{\rm lab}$ rotates in the trap at the frequency Ω in the lab frame, so does $\tilde{\psi}$ in terms of the renormalized time τ. In the limit of $t\to\infty$, τ tends to a finite value $\tau_{\rm max}$, so that $\tilde{\psi}$ is rotated by a finite angle during the ballistic expansion:

$$\Omega\tau_{\rm max}=\Omega\int_0^\infty\frac{\mathrm{d}t}{\lambda^2(t)}=\frac{\pi}{2}\frac{\Omega}{\omega(0)}\,. \tag{38}$$

Therefore $\psi_{\rm lab}$ rotates with respect to its value when the trap is switched off and its size is magnified by $\lambda(t)$.

A fourth possibility, giving direct access to the phase of the vortex, is to measure the interference fringes between a condensate with vorticity and a reference condensate with no vortex. We study this possibility as an application of the scaling solution [21]. The condensate 2 has one or several vortices and is originally centered at $\mathbf{r}=0$, the condensate 1 has no vortex and is centered initially at $\mathbf{r}=\mathbf{d}$. After ballistic expansion of the condensates the resulting density can be written:

$$\rho_{1+2}=|\rho_1^{1/2}\mathrm{e}^{\mathrm{i}m(\mathbf{r}-\mathbf{d})^2/2\hbar t}+\rho_2^{1/2}\mathrm{e}^{\mathrm{i}mr^2/2\hbar t}\mathrm{e}^{\mathrm{i}S}\mathrm{e}^{\mathrm{i}\gamma(t)}|^2 \tag{39}$$

where ρ_1 and ρ_2 are the densities of the condensates 1 and 2 respectively, S is the phase due to vorticity of the condensate 2, $\gamma(t)$ is a relative phase depending only on time; to obtain the phase terms quadratic in $\mathbf{r}$ we have used equation (33) with the asymptotic value $\dot{\lambda}/\lambda\simeq 1/t$ for $t\to\infty$. We have plotted an example of interference fringes with two vortices in Figure 3.

The above scaling result is exact only for axi-symmetry 2D traps. For a non axi-symmetric traps and for 3D situations where the confinement along z is not strong, it has been shown that approximate scaling solutions exist in the absence of a vortex [19,20]; in presence of vortices we have integrated numerically the time dependent Gross-Pitaevskii equation and found that the density experiences an approximate scaling, the magnification of the vortex being slightly larger than the one of the cloud (see also [22]).

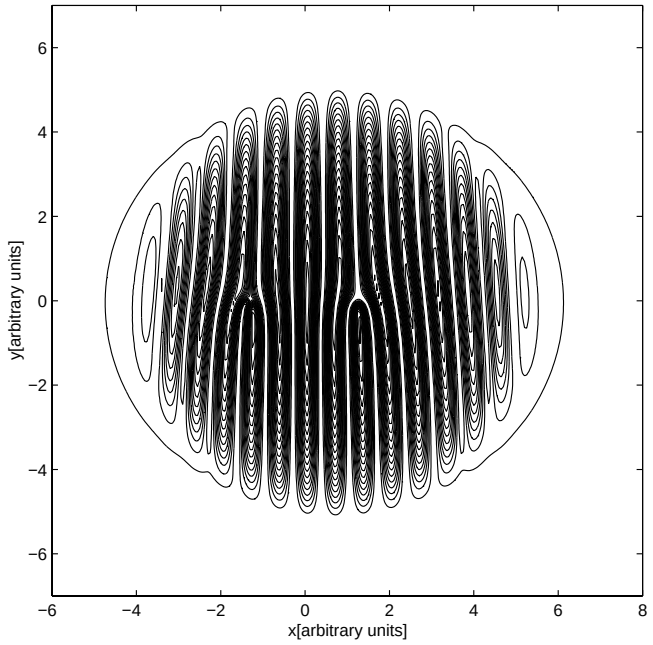

Fig. 3. Isocontours of the total density ρ_{1+2} for two ballistically expanded condensates. The condensate 2 has two vortices; it was prepared in an axi-symmetric trap with $\Omega = 0.2\omega$. The condensate 1 has no vortex and is slightly displaced along the axis x connecting the two vortex cores at time t.

6 Intuitive variational calculation

To get a better understanding of the numerical results we now proceed to an intuitive ansatz for the wavefunction with several vortices. It coincides very well with the numerical results and allows an easy construction of the minimal energy configurations with vortices. It gives a physical understanding of the stability conditions and of the structure of the solutions: a set of n vortices is equivalent to a gas of interacting particles in presence of an external potential adjusted by the rotation frequency of the trap. We restrict to the case of an axi-symmetric trap, a good approximation for weak ($< 10\%$) non-axisymmetries (see Sect. 3.2).

6.1 Ansatz for the density

To construct the ansatz we split ψ in a modulus and a phase:

$$\psi(x,y) = |\psi| \mathrm{e}^{\mathrm{i}S}. \tag{40}$$

In the Thomas-Fermi regime, the modulus in presence of n vortices appears as a slowly varying envelope given by the Thomas-Fermi approximation used in the 0-vortex case:

$$\psi_{\rm slow} = \left[\frac{\mu - m\omega^2 r^2/2}{Ng}\right]^{1/2} \tag{41}$$

with narrow holes digged by the vortices with charge $q = \pm 1$, represented by tanh functions of adjustable widths and with zeros at adjustable positions:

$$|\psi| = \psi_{\rm slow} \prod_{k=1}^{n} \tanh[\kappa_k |\mathbf{r} - \boldsymbol{\alpha}_k R|]. \tag{42}$$

The positions of the vortex cores $\boldsymbol{\alpha}_k$ are expressed in units of the Thomas-Fermi radius R of the condensate:

$$R = \sqrt{\frac{2\mu}{m\omega^2}}\,. \tag{43}$$

From Section 4.2 we expect as typical values for the inverse width of the vortex cores $\kappa_k \simeq (m\mu/\hbar^2)^{1/2}$. The chemical potential is not an independent variable but is expressed as a function of the other parameters from the normalization condition $\langle\psi|\psi\rangle = 1$; neglecting overlap integrals between the holes we get

$$\mu = \mu_0 \left[1 + 2\sum_{k=1}^{n}(1-\alpha_k^2)\frac{\ln 2}{(\kappa_k R)^2} + O\left(\frac{1}{(\kappa R)^4}\right)\right] \tag{44}$$

where $1/(\kappa R)^4 \sim (\hbar\omega/\mu)^4 \ll 1$ and where μ_0 is the Thomas-Fermi approximation for the condensate chemical potential without vortices:

$$\mu_0 = \left(\frac{m\omega^2 N g}{\pi}\right)^{1/2}. \tag{45}$$

6.2 The phase

The general form of the phase of ψ in equation (40) in presence of n vortices is:

$$S(x,y) = \sum_{k=1}^{n} q_k \theta_k + S_0(x,y) \tag{46}$$

where the integer $q_k = \pm 1$ is the vortex charge (that is the angular momentum (over $\hbar$) of the vortex k with respect to its core axis), θ_k is the polar angle of a system of Cartesian coordinates (X,Y) centered on the vortex core and S_0 is the single-valued part of the phase. The function S_0 can in principle be determined from the modulus of ψ from the continuity equation:

$$\mathrm{div}[|\psi|^2 \mathbf{v}\,] = 0. \tag{47}$$

The local velocity field $\mathbf{v}$ is related to the phase S by

$$\mathbf{v} = \frac{\hbar}{m}\boldsymbol{\nabla} S - \boldsymbol{\Omega} \wedge \mathbf{r}. \tag{48}$$

This expression is derived from the relation between the velocity operator and the momentum operator in the rotating frame, $\hat{\mathbf{v}} = \hat{\mathbf{p}}/m - \boldsymbol{\Omega} \wedge \hat{\mathbf{r}}$. Expanding the continuity equation we obtain

$$|\psi|^2 \Delta S + \boldsymbol{\nabla}|\psi|^2 \cdot \boldsymbol{\nabla} S - \frac{m\Omega}{\hbar}[x\partial_y - y\partial_x]|\psi|^2 = 0. \tag{49}$$

This can be turned into an equation for the single-valued part S_0 of the phase; because the density $|\psi|^2$ in a trap vanishes at the border of the condensate S_0 is uniquely determined (up to a constant) by the resulting equation (see Appendix); this is to be contrasted to the case of superfluid helium in a container, where the flux, not the density, vanishes at the border, which requires a boundary condition on the gradient of the phase.

Equation (49) can be solved for a non-axisymmetric trap in the absence of vortices. The solution is given by

$$S(x,y) = -\frac{m\Omega}{\hbar}\frac{\omega_x^2-\omega_y^2}{\omega_x^2+\omega_y^2}xy \tag{50}$$

which leads to a change in the energy per particle

$$\delta E = -\frac{1}{6}\mu_{\rm TF}\Omega^2\frac{(\omega_x^2-\omega_y^2)^2}{(\omega_x^2+\omega_y^2)\omega_x^2\omega_y^2} \tag{51}$$

where $\mu_{\rm TF}$ is the Thomas-Fermi approximation for the chemical potential for $\Omega = 0$, $\mu_{\rm TF} = (m\omega_x\omega_y N g/\pi)^{1/2}$ [23]. As can be seen in Figure 2 this prediction is in good agreement with our numerical results.

In presence of vortices the equation for S is more difficult to solve analytically. From now on we consider the case of an axi-symmetric trap, as the energy ordering of the vortices solutions is not affected for weak ($< 10\%$) non-axisymmetries (see Sect. 3.2). For a single vortex at the center of the trap one can see that $S_0 = 0$ solves equation (49). From the spatial dependence of the phase obtained numerically (Sect. 3.2) for a displaced vortex or several vortices we have identified the following heuristic ansatz, obtained in setting $\omega_x = \omega_y = \omega$ in equation (50):

$$S_0(x,y) \equiv 0 \tag{52}$$

that we will use in the remaining part of the section.

6.3 Further approximations for the mean energy

In the calculation of the mean energy, we make some further approximations in the spirit of the ansatz equation (42). The reader not interested by these more technical considerations can proceed to the next subsection.

The kinetic energy involves an integral of the gradient squared of the wavefunction:

$$|\boldsymbol{\nabla}\psi|^2 = |\psi|^2\left[(\boldsymbol{\nabla}\ln|\psi|)^2 + (\boldsymbol{\nabla}S)^2\right]. \tag{53}$$

For the gradient of the modulus of ψ we neglect the variation of the slow envelope $\psi_{\rm slow}$:

$$\boldsymbol{\nabla}\ln|\psi| \simeq \sum_{k=1}^{n}\kappa_k\frac{\tanh'}{\tanh}[\kappa_k|\mathbf{r}-\boldsymbol{\alpha}_k R|]\,(\mathbf{e}_r)_k \tag{54}$$

where $(\mathbf{e}_r)_k = (\mathbf{r}-\boldsymbol{\alpha}_k R)/|\mathbf{r}-\boldsymbol{\alpha}_k R|$. The terms in this sum are peaked around the vortex cores; assuming a separation between the vortex cores much larger than their width, we neglect all the crossed terms in the square of equation (54).

Consider now the second term in equation (53). The gradient squared of S involves diagonal terms $(\boldsymbol{\nabla}\theta_k)^2$ and non-diagonal terms $\boldsymbol{\nabla}\theta_k\cdot\boldsymbol{\nabla}\theta_{k'}$; the modulus squared of ψ involves holes with a density varying as $1-\tanh^2 = \mathrm{sech}^2$. In the following we keep the sech^2 for the vortex k only if it is multiplied by $(\boldsymbol{\nabla}\theta_k)^2$, a quantity diverging in the center of the core; the other terms lead to converging integrals smaller by a factor $(\mu/\hbar\omega)^2$, which is the inverse surface of a vortex core ($\int \mathrm{d}^3\mathbf{r}\ |\psi_{\rm slow}|^2\mathrm{sech}^2\kappa r \propto 1/(\kappa R)^2$). This finally leads to

$$E_{\rm kin} \simeq \frac{\hbar^2}{2m}\int \mathrm{d}^2\mathbf{r}\ |\psi_{\rm slow}|^2\left[\sum_{k=1}^{n}\tanh^2[\kappa_k|\mathbf{r}-\boldsymbol{\alpha}_k R|](\boldsymbol{\nabla}\theta_k)^2 + \kappa_k^2\left(\tanh'[\kappa_k|\mathbf{r}-\boldsymbol{\alpha}_k R|]\right)^2 + \sum_{k=1}^{n}\sum_{k'\neq k} q_k q_{k'}\boldsymbol{\nabla}\theta_k\cdot\boldsymbol{\nabla}\theta_{k'}\right]. \tag{55}$$

In the same spirit we simplify the contribution of $-\Omega L_z$ to the energy:

$$E_{\rm rot} = -\hbar\boldsymbol{\Omega}\cdot\int \mathrm{d}^2\mathbf{r}\ |\psi|^2\mathbf{r}\wedge\boldsymbol{\nabla}S \tag{56}$$

$$\simeq -\hbar\boldsymbol{\Omega}\cdot\int \mathrm{d}^2\mathbf{r}\ |\psi_{\rm slow}|^2\mathbf{r}\wedge\sum_{k=1}^{n}q_k\boldsymbol{\nabla}\theta_k. \tag{57}$$

In the potential energy

$$E_{\rm pot} = \int \mathrm{d}^2\mathbf{r}\ |\psi|^2\left[\frac{1}{2}m\omega^2 r^2 + \frac{1}{2}Ng|\psi|^2\right] \tag{58}$$

we will neglect in $|\psi|^4$ products of sech^2 coming from different vortex cores.

6.4 A more physical form of the mean energy

After the approximations detailed in the previous subsection the mean energy in presence of n vortices is a sum of one-vortex self energies and binary interaction energies between the vortices:

$$E = \frac{2}{3}\mu_0 + \sum_{k=1}^{n}W(\boldsymbol{\alpha}_k,\kappa_k) + \frac{1}{2}\sum_{k=1}^{n}\sum_{k'\neq k}V(\boldsymbol{\alpha}_k,\boldsymbol{\alpha}_{k'}). \tag{59}$$

Equation (59) allows to interpret a system with n vortices as a gas of "particles" with binary interactions; the form of the interaction potential obtained here is valid for a separation between the "particles" larger than the size $1/\kappa$ of the vortex cores. The vortex self-energy is

$$W(\boldsymbol{\alpha},\kappa) = \frac{(\hbar\omega)^2}{\mu_0}\left\{\frac{1}{2}+(\alpha^2-1)\left[C-\ln\kappa R-\frac{1}{2}\ln(1-\alpha^2)\right]\right\} - q\hbar\Omega\left[(1-\alpha^2)^2\right] + \frac{\mu_0}{3}\left[(4\ln 2-1)\frac{(1-\alpha^2)^2}{(\kappa R)^2}\right] \tag{60}$$

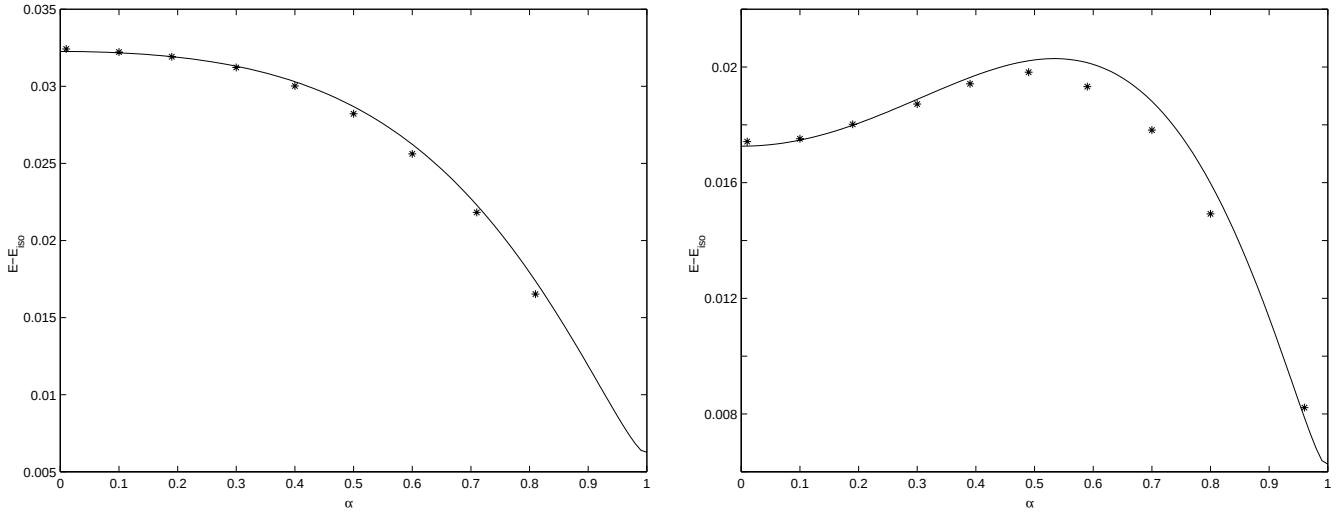

Fig. 4. Self-energy of a vortex in an axisymmetric trap as function of the distance αR of the core from the trap center, for $\mu_0 \simeq 80\hbar\omega$. (a) $\Omega = 0.03\omega$ and (b) $\Omega = 0.045\omega$. The solid lines are given by the analytical prediction $W(\boldsymbol{\alpha})$. The stars are obtained numerically. The critical frequencies defined in the text are $\Omega_{\rm c} \simeq 2\Omega_{\rm stab} \simeq 0.06\omega$. $E_{\rm iso}$ is the energy of the 0-vortex solution and the unit of energy is $\hbar\omega$.

where $C = 0.495\,063$. The lines in equation (60) correspond successively to $E_{\rm kin}$, $E_{\rm rot}$ and $E_{\rm pot}$. This can be seen as an effective potential for the vortices. One can check that the part of W independent of Ω expels the vortex core from the trap center, whereas the part proportional to Ω provides a confinement of the vortex core (see the following subsection).

The vortex interaction potential is given by

$$\frac{1}{2}V(\boldsymbol{\alpha},\boldsymbol{\beta}) = \frac{\hbar^2}{2m}q_\alpha q_\beta \int {\rm d}^2\mathbf{r}\ |\psi_{\rm slow}|^2 \boldsymbol{\nabla}\theta_{\boldsymbol{\alpha}R}\cdot\boldsymbol{\nabla}\theta_{\boldsymbol{\beta}R}. \quad (61)$$

This interaction term is equivalent to the one found in the homogeneous case and describes a repulsive interaction for vortices rotating in the same direction ($q_\alpha q_\beta > 0$) and is attractive for vortices with opposite charges [9]. An attractive interaction will lead to the coalescence and consequently annihilation of vortices with opposite charges. Therefore we find in stationary systems always vortices with equal charges.

As the interaction potential $V(\boldsymbol{\alpha},\boldsymbol{\beta})$ does not depend on the parameters κ we can optimize separately the self-energy part with respect to κ and find

$$(\kappa R)^2 = \xi^2(1-\alpha^2)\left(\frac{\mu_0}{\hbar\omega}\right)^2 \quad (62)$$

where $\xi = [(2/3)(4\ln 2 - 1)]^{1/2} \simeq 1.087\,07$. By rewriting the above equation as

$$\frac{\hbar^2\kappa^2}{m} = \frac{1}{2}\xi^2\left[\mu - \frac{1}{2}m\omega^2(\alpha R)^2\right] \quad (63)$$

we find that κ^2 is proportional to the local chemical potential at the position αR of the vortex core. We finally get the explicit form for the self energy as

$$W(\boldsymbol{\alpha}) = \frac{(\hbar\omega)^2}{\mu_0}\left\{\frac{1}{2} + (1-\alpha^2)\left[\frac{2\ln 2 + 1}{3} + \ln\frac{\nu\mu_0}{\hbar\omega} + \ln(1-\alpha^2) - q\frac{\Omega\mu_0}{\hbar\omega^2}(1-\alpha^2)\right]\right\} \quad (64)$$

where $\nu = 0.493\,12$.

6.5 Case of a single vortex: critical frequencies

In Figure 4 we have plotted the self-energy of a vortex as a function of the displacement of the core from the trap center, for different values of the rotation frequency Ω. The analytical prediction coincides very well with the numerical value [24].

For $\Omega = 0$ the position of the vortex at the trap center gives an energy maximum. For $\Omega > 0$ the rotation of the trap provides an effective confinement of the vortex core at the center of the trap for positive charges q (see the term proportional to Ω in Eq. (64)); from now one we therefore take all the charges q_k to be equal to $+1$. For a large enough Ω we reach a situation where a vortex at the trap center corresponds to a local energy minimum, by further increasing Ω the vortex state at the trap center becomes a global minimum with energy less than the condensate without vortex.

The above suggests that we have to distinguish two critical rotation frequencies: the first one defines the frequency $\Omega_{\rm stab}$ above which the vortex is a local minimum of energy. Above the frequency $\Omega_{\rm c}$ the single vortex solution has an energy lower than the condensate without vortex.

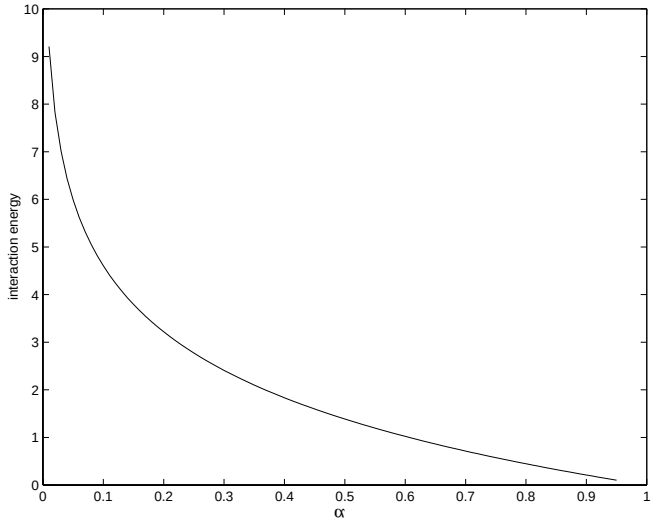

Fig. 5. Interaction energy between a vortex at the center of the trap and a vortex at a distance αR from the center, as given by the analytical formula equation (67) for V. The trap is axisymmetric; the unit of energy is $(\hbar\omega)^2/\mu_0$.

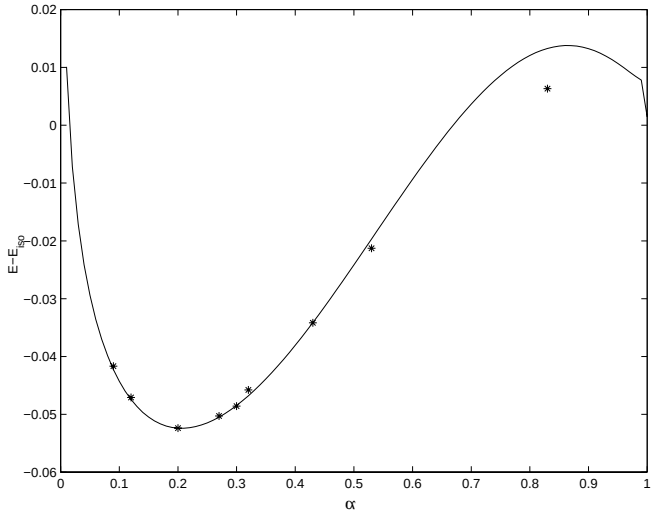

Fig. 6. Energy of a system of two vortices symmetrically displaced by $\pm\alpha R$ from the trap center, as function of the displacement α, for $\Omega = 0.1\omega$ and $\mu_0 \simeq 80\hbar\omega$. Solid line: analytical result. Stars: numerics. The trap is axisymmetric; $E_{\rm iso}$ is the energy of the 0-vortex solution and the unit of energy is $\hbar\omega$.

We calculate $\Omega_{\rm stab}$ from the condition $\mathrm{d}^2W/\mathrm{d}\alpha^2 = 0$ at $\alpha = 0$ and $\Omega_{\rm c}$ from the condition $W = 0$ at $\alpha = 0$:

$$\Omega_{\rm c} = \frac{\hbar\omega^2}{\mu_0} \ln\left[\frac{C'\mu_0}{\hbar\omega}\right] \tag{65}$$

$$\Omega_{\rm stab} = \frac{\hbar\omega^2}{2\mu_0} \ln\left[\frac{C'\mathrm{e}^{1/2}\mu_0}{\hbar\omega}\right] \tag{66}$$

where $C' = \mathrm{e}^{(2\ln 2+1)/3+1/2}\nu \simeq 1.8011$. As we are in the regime $\mu_0 \gg \hbar\omega$, $\Omega_{\rm c}$ is approximately twice $\Omega_{\rm stab}$ [25]. Our prediction for $\Omega_{\rm c}$ scales as $(\log\mu_0)/\mu_0$ as in [15].

6.6 Case of several vortices

By integrating equation (61) we get an explicit form for the vortex interaction potential for vortices with equal charges:

$$V(\boldsymbol{\alpha},\boldsymbol{\beta}) = \frac{(\hbar\omega)^2}{\mu_0}\left\{\alpha^2+\beta^2-1-|\boldsymbol{\alpha}\wedge\boldsymbol{\beta}|\arctan\left[\frac{|\boldsymbol{\alpha}\wedge\boldsymbol{\beta}|}{(1-\boldsymbol{\alpha}\cdot\boldsymbol{\beta})}\right] + \frac{1}{2}(1-\boldsymbol{\alpha}\cdot\boldsymbol{\beta})\log\left[\frac{1-2\boldsymbol{\alpha}\cdot\boldsymbol{\beta}+\alpha^2\beta^2}{|\boldsymbol{\alpha}-\boldsymbol{\beta}|^4}\right]\right\}. \tag{67}$$

At short distances between the two vortex cores the logarithmic term in the above expression dominates, leading to a repulsive potential $\sim -2(1-\boldsymbol{\alpha}\cdot\boldsymbol{\beta})\log|\boldsymbol{\alpha}-\boldsymbol{\beta}|(\hbar\omega)^2/\mu_0$. In Figure 5 we plot the interaction energy between a vortex at the center of the trap and one of equal charge displaced by αR; the interaction is purely repulsive. A conclusion which essentially holds as well for arbitrary vortex positions. In Figure 6 we show the total (interaction + self-energy) for two vortices symmetrically displaced from the trap center, as function of the displacement; the analytical prediction coincides again very well with the numerical results [24]. To obtain the equilibrium distance between the two vortex cores one minimizes the total energy over α in Figure 6.

To get the minimal energy configurations as function of the rotation frequency of the trap, we minimize our analytical prediction for the energy over the positions of the $n = 1, 2, \ldots$ vortex cores. The result is shown in Figure 7. Each curve corresponds to a fixed value of n; it starts at $\Omega = \Omega_{\rm stab}(n)$ (for $\Omega < \Omega_{\rm stab}(n)$ there is no local minima of energy with n vortices); it becomes the global energy minimum for $\Omega = \Omega_{\rm c}(n)$. We have plotted these two critical frequencies as function of n in Figure 8.

We have also given numerical results (circles) in Figure 7. Even if there is good agreement between analytical and numerical results, we still need a numerical calculation to check the stability of the solutions; our simple analytical ansatz is indeed not sufficient to predict the destabilization of a given vortex configuration at high Ω, a phenomenon studied with a numerical calculation of the Bogoliubov spectrum for a single vortex in [26].

For a fixed value of the number of vortices n there may exist local minima of energy, in addition to the global minimum plotted in Figure 7, a situation known from superfluid helium [4]. *E.g.* for $n = 6$ (see Fig. 9) the global minimum of energy is given by a configuration with six vortex cores on a circle; there exists also a local minimum of energy with one vortex core at the center of the trap and five vortex cores on a circle. The energy difference per particle between the two configurations is very small, $\delta E \simeq 0.002\hbar\omega$ for the parameters of the figure and probably beyond the accuracy of our variational ansatz. For relatively large rotation frequencies Ω one can find local minima of energy configurations with many vortices (see [4] for superfluid helium); we plot two configurations

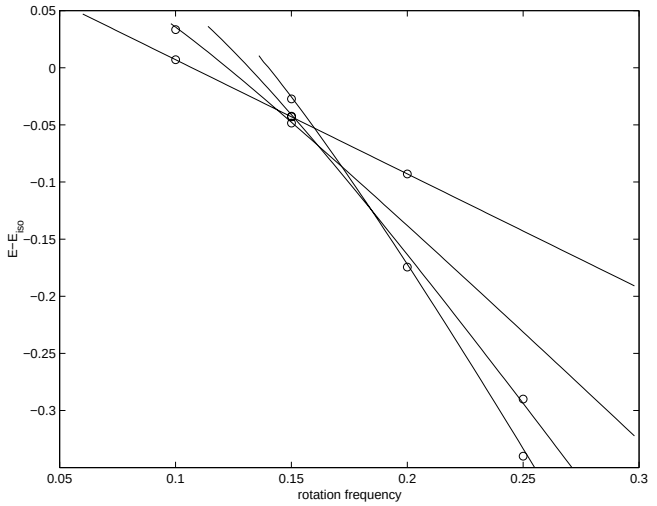

Fig. 7. Local minima of energy with n vortices in an axisymmetric trap as function of the rotation frequency Ω of the trap in units of the trap frequency ω. The chemical potential μ_0 is approximately $40\hbar\omega$. Note that for a fixed n we kept only the local minimum with the lowest energy. The circles are numerical results. The reference of energy is $E_{\rm iso}$, the energy per particle in the absence of vortex, and the unit of energy is $\hbar\omega$. The lines with increasing absolute value of the slope correspond to $n = 1, \ldots, 4$ vortices respectively.

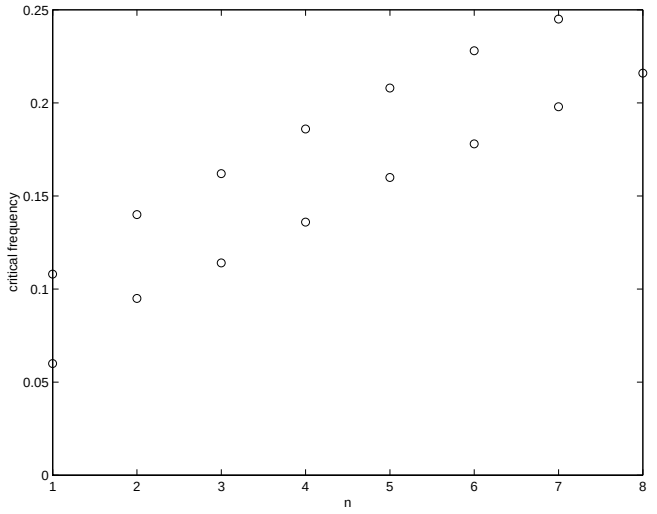

Fig. 8. Critical frequencies $\Omega_{\rm stab}(n)$ and $\Omega_{\rm c}(n)$ (see text) obtained from the analytical ansatz as function of the number of vortices. The chemical potential μ_0 is approximately $40\hbar\omega$ and the unit for Ω is the trap frequency ω.

with 18 vortices in Figure 10, with an energy difference $\delta E = 0.0034\hbar\omega$.

In estimating the physical relevance of these energy differences one should keep in mind that $N\delta E$ matters, rather than δE, where N is the number of particles in the condensate: *e.g.* at a finite temperature T the ground energy configuration is statistically favored as compared to the metastable one when $N\delta E \gg k_{\rm B}T$.

7 Vortices in a 3D configuration

We have extended the numerical calculation to the case of a 3D cigar-shaped trap, that is with a confinement weaker along the rotation axis than in the $x-y$ plane. Even in this case rotation of the trap can stabilize the vortex. We show in Figure 11 density cuts of a solution with 5 vortices; the vortex cores are almost straight lines in the considered Thomas-Fermi regime, except at vicinity of the borders of the condensate. As in Section 6 the core diameter is determined by the local chemical potential in the gas.

This suggests that our 2D ansatz (Sect. 6) can be generalized to 3D situations, with $\boldsymbol{\alpha}_k$ and κ_k depending on z.

8 Conclusion and perspectives

We have presented in this paper an efficient numerical algorithm and a heuristic variational ansatz to determine the local minima energy configurations for a Bose-Einstein condensate strongly confined along z and subject to a rotating harmonic trap in the $x-y$ plane.

Our results can be used as a first step towards finite temperature calculations. Interesting problems are *e.g.* the critical temperature for the vortex formation and the Magnus forces induced by the non-condensed particles on the vortex core [27].

We acknowledge useful discussions with Sandro Stringari and Dan Rokhsar. We thank J. Dalibard for useful comments on the manuscript. We thank the ITP at Santa Barbara for its hospitality and the NSF for support under grant No. PHY94-07194. This work was partially supported by the TMR Network "Coherent Matter Wave Interactions", FMRX-CT96-0002.

Appendix A: Uniqueness of the phase from the continuity equation in a trap

Consider two solutions S_1 and S_2 of the continuity equation:

$$\mathrm{div}[|\psi|^2 \boldsymbol{\nabla} S] = \frac{m\Omega}{\hbar}(x\partial_y - y\partial_x)|\psi|^2. \qquad \text{(A.1)}$$

S_1 and S_2 correspond to the same positions of the vortex cores, so that their difference S_{12} is a single-valued function of the position, solving

$$\mathrm{div}[|\psi|^2 \boldsymbol{\nabla} S_{12}] = 0. \qquad \text{(A.2)}$$

To show that in the case of a trapped condensate S_{12} is a constant we consider the following integral

$$I = \iint_{\mathcal{A}} \mathrm{div}[|\psi|^2 S_{12} \boldsymbol{\nabla} S_{12}] \qquad \text{(A.3)}$$

where the integration runs over the area $\mathcal{A}$ of the condensate.

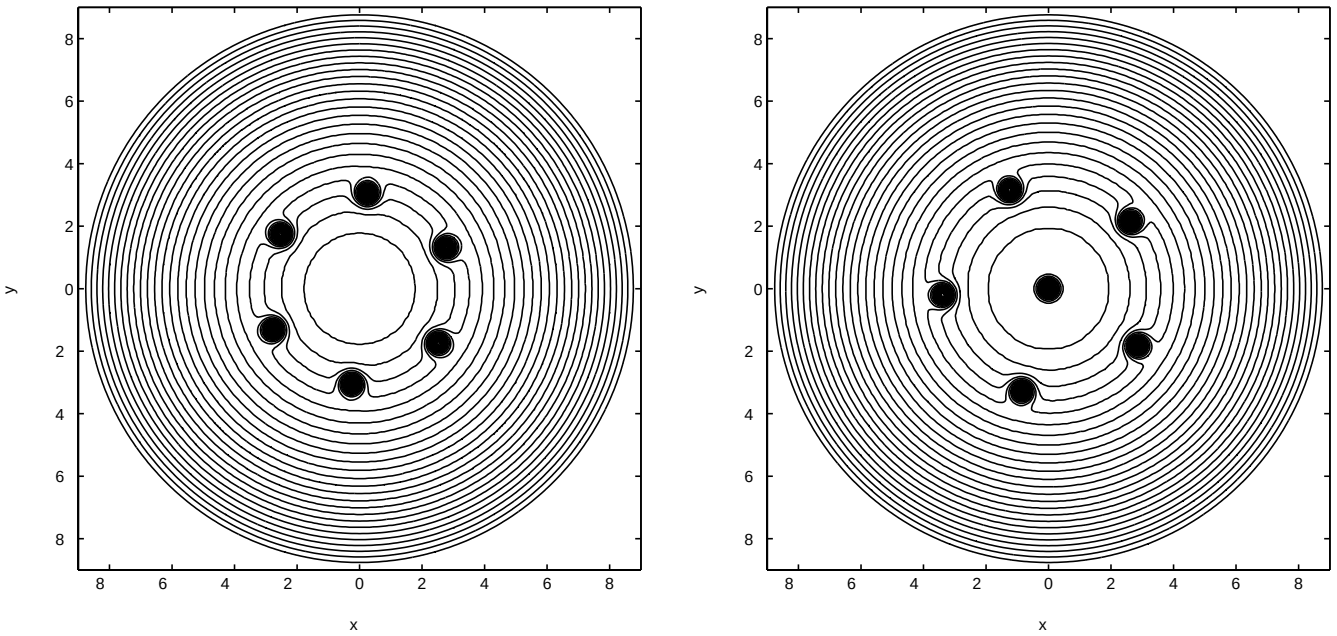

(a) (b)

Fig. 9. In an axi-symmetric trap with $\Omega = 0.3\omega$ and $\mu_0 \simeq 40\hbar\omega$, different configurations of 6 vortices corresponding to a local minimum of energy: (a) 6 vortices on a circle, with an energy per particle $E = E_{\rm iso} - 0.5910\hbar\omega$; (b) one vortex at the center and 5 vortices on a circle, with $E = E_{\rm iso} - 0.5890\hbar\omega$. $E_{\rm iso}$ is the energy per particle in the absence of vortex. The unit of length is $(\hbar/m\omega)^{1/2}$.

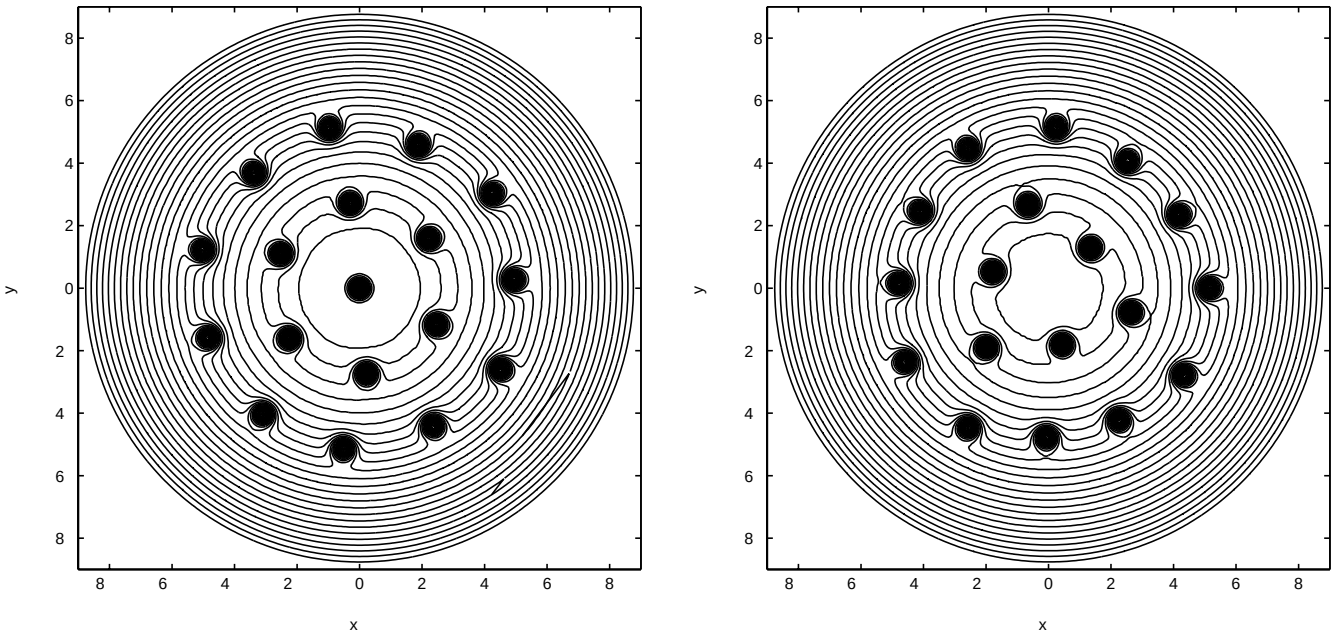

(a) (b)

Fig. 10. In an axi-symmetric trap with $\Omega = 0.5\omega$ and $\mu \simeq 40\hbar\omega$, different configurations of 18 vortices corresponding to a local minimum of energy: (a) with one vortex at the center $E = E_{\rm iso} - 2.3988\hbar\omega$, this is the global minimum of energy; (b) without vortex core at the center; the energy per particle is slightly higher, $E = E_{\rm iso} - 2.3954\hbar\omega$. $E_{\rm iso}$ is the energy per particle in the absence of vortex. The unit of length is $(\hbar/m\omega)^{1/2}$.

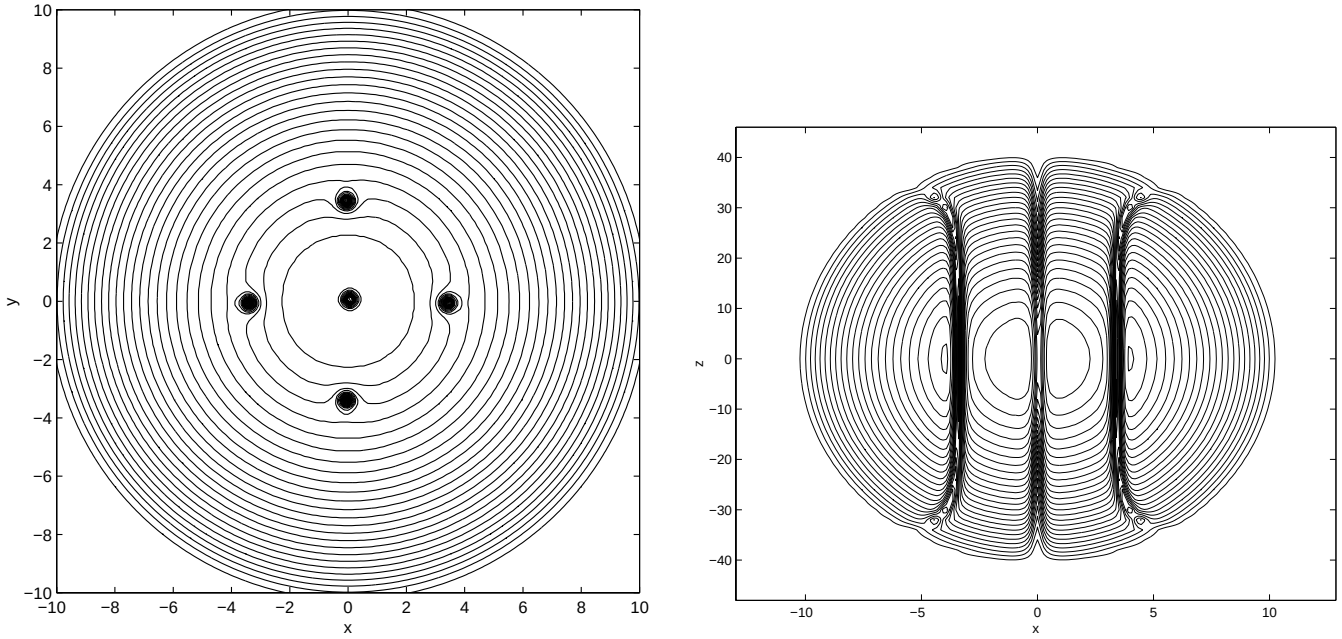

(a) (b)

Fig. 11. A local minimum energy solution in 3D with 5 vortices obtained from the numerical evolution in complex time. The trapping frequencies are in the ratio $\omega_x = \omega_y = 4\omega_z$. The chemical potential is $53.7\hbar\omega_{x,y}$. The trap is rotated at a frequency $\Omega = 0.25\omega_{x,y}$. (a) Isocontours for a cut of the density in the plane $z = 0$, showing the 5 vortex cores. (b) Isocontours for a cut of the density in the $x-z$ plane, showing the dependence with z of the vortex cores. The unit of length is $(\hbar/m\omega_{x,y})^{1/2}$.

First, we transform I using Gauss's formula into an integral over the border $\bar{\mathcal{A}}$ of the condensate:

$$I = \int_{\bar{\mathcal{A}}} |\psi|^2 S_{12} \boldsymbol{\nabla} S_{12} \cdot \mathbf{n} = 0 \tag{A.4}$$

which vanishes as $|\psi|^2 = 0$ on the border of the condensate.

Second, we expand the integrand of I as

$$\mathrm{div}[|\psi|^2 S_{12} \boldsymbol{\nabla} S_{12}] = S_{12} \mathrm{div}[|\psi|^2 \boldsymbol{\nabla} S_{12}] + |\psi|^2 (\boldsymbol{\nabla} S_{12})^2. \tag{A.5}$$

The first term in the right hand side vanishes in virtue of the continuity equation. Therefore

$$0 = I = \int\!\!\int_{\mathcal{A}} |\psi|^2 (\boldsymbol{\nabla} S_{12})^2. \tag{A.6}$$

As the integrand is positive this implies $\boldsymbol{\nabla} S_{12} = \mathbf{0}$, that is $S_{12} = constant$.

References

1. M.H. Anderson, J.R. Ensher, M.R. Matthews, C.E. Wieman, E.A. Cornell, Science **269**, 198 (1995); K.B. Davis, M.O. Mewes, M.R. Andrews, N.J. van Druten, D.S. Durfee, D.M. Kurn, W. Ketterle, Phys. Rev. Lett. **75**, 3969 (1995); C.C. Bradley, C.A. Sackett, R.G. Hulet, Phys. Rev. Lett. **78**, 985 (1997).
2. F. Dalfovo, S. Giorgini, L. Pitaevskii, S. Stringari, Rev. Mod. Phys. **71**, 463 (1999).
3. L. Onsager, Nuovo Cimento **6**, 249 (1949).
4. R.J. Donnelly, *Quantized vortices in helium II* (Cambridge, 1991).
5. A.J. Leggett, Topics in superfluidity and superconductivity, in *Low Temperature Physics*, edited by M.J.R. Hoch, R.H. Lemmer (Springer Verlag, 1992).
6. M. Olshanii, M. Naraschewski, `cond-mat/9811314`; K.G. Petrosyan, Li You, Phys. Rev. A **59**, 639 (1999).
7. R. Dum, I. Cirac, M. Lewenstein, P. Zoller, Phys. Rev. Lett. **80**, 2972 (1998).
8. B. Jackson, J.F. McCann, C.S. Adams, Phys. Rev. Lett. **80**, 3903 (1998).
9. This was studied in the homogeneous case by S. Fetter, Phys. Rev. A **148**, 429 (1965); G.B. Hess, Phys. Rev. **161**, 189 (1967).
10. D.A. Butts, D.S. Rokhsar, Nature **397**, 327 (1999).
11. D.M. Stamper-Kurn, M.R. Andrews, A.P. Chikkatur, S. Inouye, H.-J. Miesner, J. Stenger, W. Ketterle, Phys. Rev. Lett. **80**, 2027 (1998).
12. We assume here that the spatial extension of the ground state of the harmonic oscillator along z remains much larger than the scattering length a, otherwise the derivation of g in 2D is more complicated; see *e.g.* M. Olshanii, Phys. Rev. Lett. **81**, 938 (1998) for a calculation of g_{1D} from g_{3D} in presence of a ultra-strong $x-y$ confinement.
13. We disregard here the zero energy mode coming from the arbitrariness of the global phase of ψ. This mode is absent in a Bogoliubov treatment preserving the $U(1)$ symmetry of the problem, see C. Gardiner, Phys. Rev. A **56**, 1414 (1997); Y. Castin, R. Dum, Phys. Rev. A **57**, 3008 (1998).

14. D.S. Rokhsar, Phys. Rev. Lett. **79**, 2164 (1997).
15. F. Dalfovo, S. Stringari, Phys. Rev. A **53**, 2477 (1996).
16. H. Pu, C.K. Law, J.H. Eberly, N. Bigelow, Phys. Rev. A **59**, 1533 (1999); N. Bigelow (private communication).
17. R.J. Dodd, K. Burnett, M. Edwards, C.W. Clark, Phys. Rev. A **56**, 587 (1997); F. Zambelli, S. Stringari, Phys. Rev. Lett. **81**, 1754 (1998).
18. An idea along this line can be found in E.V. Goldstein, E.M. Wright, P. Meystre, Phys. Rev. A **58**, 576 (1998).
19. Y. Kagan, E.L. Surkov, G. Shlyapnikov, Phys. Rev. A. **54**, R1753 (1996); L. Pitaevskii, A. Rosch, Phys. Rev. A **55**, R835 (1997).
20. Y. Castin, R. Dum, Phys. Rev. Lett. **77**, 5315 (1996).
21. S. Stringari (private communication); a purely numerical approach to calculate the interference fringes was taken in E.L. Bolda, D.F. Walls, Phys. Rev. Lett. **81**, 5477 (1998).
22. E. Lundh, C.J. Pethick, H. Smith, Phys. Rev. A **58**, 4816 (1998).
23. S. Fetter (unpublished).
24. The numerical results for the energy curves are obtained as follows. We start with ψ given by the ansatz for one or several vortices displaced from the trap center and evolve it in complex time. We observe that the positions of the vortices evolve very slowly whereas the other variables such as the phase relax rapidly to a quasi steady-state. This allows to define an energy as function of the positions of the cores.
25. In the 3D calculation of S. Fetter, `cond-mat/981148`, it is found that $\Omega_{\rm c} = (5/3)\Omega_{\rm stab}$.
26. T. Isoshima, K. Machida, `cond-mat/9811367`.
27. E.B. Sonin, Phys. Rev. B **55**, 485 (1997).